Characterization of Ball-Milled Bamboo-Based Activated Carbon Treated with $KMnO_4$ and KOH as Activating Agents

Qanytah,[a,b] Khaswar Syamsu,[b] Farah Fahma,[b] and dan Gustan Pari [c]

Bamboo-based activated carbon was made using the activating agents KOH and $KMnO_4$ at high temperature. This study examined the ability of unmilled and ball-milled bamboo activated using KOH or $KMnO_4$ to fulfil the activated carbon standard parameters. Chemical activation was done using KOH and $KMnO_4$ at 2.5% and 5% concentration, heated at 800 °C, and steamed for 1 hour. Sample size was reduced to 500 nm using high energy ball-milling at 500 rpm for 80, 150, or 180 min. Analysis included the yield, water content, ash content, volatile matter content, burn-off weight percentage, morphology analysis, functional groups (Fourier transform infrared spectroscopy, FTIR), crystallinity analysis (X-ray diffraction, XRD), and Brunauer, Emmett, and Teller (BET) analysis. Ball-milling treatment for 150 min produced activated carbon of 449 nm in size and a particle distribution index (PDI) score of 0.66. Ball milled activated carbon from the experiment had a pore radius ranging from 1.18 to 2.49 nm. The activated carbon that met the criteria of ANSI/AWWA B604-12 (2012) standard for moisture content, iodine number, and JIS K 1474 (1967) standard for methylene blue adsorption level and surface area were milled activated carbon with activator $KMnO_4$ 2.5%.

Keywords: Activation; Activated carbon; Ball mill; Bamboo; $KMnO_4$; KOH

Contact information: a: Indonesian Center for Agricultural Postharvest Research and Development, Bogor, Indonesia; b: Department of Agroindustrial Technology, Faculty of Agricultural Engineering and Technology, IPB University (Bogor Agricultural University), Bogor, Indonesia; c: Forest Products Research and Development Center, Ministry of Environment and Forestry, Bogor, Indonesia; Corresponding author: khaswars@yahoo.com

INTRODUCTION

Bamboo is carbon material that has potential to produce activated carbon because it is available in abundance in Indonesia, where around 60 different types of bamboo are found. It has the advantages of short growth cycle (3 to 5 years), self-reproduction, and low cost in maintenance (Chen *et al.* 2019). According to Kant (2010), bamboo produces as much as 20 to 40 tons/hectare of lignocellulosic biomass annually, and the yield is 73% higher than that of wood plants. It has more than 90% carbon and oxygen ratio from its total weight.

Activated carbon is a highly effective adsorbent for different kinds of organic (and inorganic pollutants in the liquid and gas phases (Kazmierczak *et al.* 2013). Organic compounds include humic acids, fulvic acids, carbohydrates, proteins, and carboxylic acids (Frimmel *et al.* 2002). Pollutants of interest have included metal ions (Reddad *et al.* 2002) such as copper, cadmium, chromium, nickel, zinc, and lead (Giraldo and Piraján 2008), as well as chemicals such as ammonia (NH_3) (Gonçalves *et al*. 2011), and dyes (Sivakumar *et al*. 2012).

The preparation of activated carbon involves two steps: carbonization and activation. The goal of carbonization is to enrich the carbon content and at the same time to develop the initial porosity. Bamboo charcoal is the carbonaceous residue of bamboo left after heating bamboo in the absence of oxygen at temperatures of roughly 400 °C. The carbonization process is very important in the preparation of AC, as this process will determine the imprint effect on the final product. This is the reason why it is important to select the carbonization parameters in order to produce the required quality of the final AC. In the carbonization process there are several parameters that would affect the structure, and one of these is carbonization temperature.

The adsorption level and characteristics of the activated carbon depend on the physical and chemical nature of the precursor and activation technique (Ahmed *et al.* 2012). Activation is done physically and chemically (Wang *et al.* 2017) using activating agents such as CO_2 (Song *et al.* 2013), water vapour (Deiana *et al.* 2008), KOH (Sun *et al.* 2008), H_3PO_4 (Sun *et al.* 2016), $ZnCl_2$ (Boudrahem *et al*. 2011), and $CaCl_2$ (Liu *et al*. 2016).

Physical and chemical activation are intended to break the hydrocarbon chain or by oxidizing surface molecules to enlarge the activated carbon pore. Chemical activation produces more porous carbon with higher specific surface area and larger pore volume (Song *et al.* 2013). Micropores in carbon contribute to a high specific adsorption capacity (Raymundo-Piñero *et al*. 2006), especially pores with sub-nanometer size (0.7 nm) (Chmiola *et al*. 2008; Galhena *et al*. 2016).

Chemical activation is conducted using activating agents. KOH is a strong reagent. It catalyses the oxidation reaction such that more carbon atoms on the surface are oxidized, widening the pore structures (Abdul Khalil *et al.* 2013). There has been research on the optimal concentration of KOH solution as activating agent for different carbon materials (Abdul Khalil *et al.* 2013; Nagaraju *et al.* 2016; Zhang *et al.* 2019). The research on the use of $KMnO_4$ as activating agent was conducted on granular activated carbon (Rathnayake *et al*. 2017) to find out the impact of the concentration of the $KMnO_4$ solution (Pang *et al*. 2015; Zhang *et al*. 2017).

The ability of activated carbon to serve as an adsorber is dependent on various properties (Aygun *et al.* 2003), namely, pore structure, surface area, and surface chemistry. Chemical activation using KOH or $KMnO_4$ modifies the pore structures. One method to enlarge the contact surface area is by reducing the size of the activated carbon particle. Ball milling is a processing method that mechanically reduces the particle size of solids to ultrafine scale (nano size) particles (Lyu *et al*. 2018). Ultrafine particles have a high surface area and volume ratio, which makes them more reactive.

A few workers noted that ball milling can greatly increase the adsorption capacity of activated carbon by increasing its surface area (Peterson *et al.* 2012; Lyu *et al.* 2017, 2018). However, ball-milled activated carbon is nano-sized, and its mobility with water is of potential environmental and human health concern if not stabilized in a matrix material (Lam *et al.* 2006; Helland *et al.* 2007). The further purpose of this activated carbon production was to use it in an ethylene adsorber paper through impregnation of the activated carbon into the paper matrix. The idea is that the nanosized nature of the material will not become a problem since it will be stabilized in a matrix material.

This study compared the ability of un-milled and ball-milled bamboo activated carbon, activated using KOH or $KMnO_4$, to obtain the activated carbon that fulfils standard parameters.

EXPERIMENTAL

Materials

The material used for this study was Betung bamboo (*Dendrocalamus asper*), and the chemicals used were $KMnO_4$, HCl, KOH provided from PT. Merck Indonesia Tbk, Jakarta, KOH, and other chemicals for analysis.

Methods

Production of the activated carbon

Bamboo with the size of 2.5 × 2.5 × 1.0 cm was placed in a furnace at 400 °C for 4 h and then crushed to pass through a 30-mesh screen. It was activated using 2 activation methods, physical activation and chemical activation using the activating agents KOH and $KMnO_4$. Physical activation was conducted using heat in a reactor to reach 800 °C for 1 h, and then the mixture was steamed for 1 h. Chemical activation was conducted by soaking 100 gram charcoal in activating agents KOH or $KMnO_4$ solution of 5% and 2.5% concentration, for 24 h. After drying, charcoal was placed into a reactor to reach 800 °C for 1 h, and then the mixture was steamed for 1 h. The resulted activated carbon was cooled, soaked with 1% HCl for 1 h, and washed with distilled water to remove the chloride residue (Garcia-Garcia 2002).

To acquire activated carbon with a 500 nm size, the sample size was reduced using high-energy ball-milling (Fritsch, pulverisette 7 premium line). Fifty grams of activated carbon was milled in the chamber at 500 rpm for 80, 150, and 180 min, which is a modification of the Shan *et al*. (2016) method. Activated carbon particle size was measured based on particle distribution index (PDI), in which the score of less than 0.7 indicates homogenous sample size (Bera 2015; Sarmah *et al.* 2020).

Measurements and observations of activated carbon parameters

The parameters of activated carbon examined were yield, water content, ash content, volatile matter content, burn-off weight percentage, iodine number, methylene blue adsorption, and Brunauer, Emmett, and Teller (BET) surface analysis. Pyrolysis gas chromatography/mass spectrometer (Py–GC/MS; Shimadzu GCMS-QP 2010, Kyoto, Japan) was used to analyse the functional group distribution of samples. The volatile fragments were analysed by comparing the results with previous reports and by fitting with mass spectra in the NIST spectral libraries.

Activated carbon morphology was observed using scanning electron microscopy (SEM; EVOIMA10, Zeiss, Cambridge, UK). Activated carbon was placed on the specimen holder and sputter-coated with gold at 20 mA sputter current for 60 seconds. The sample was observed with a voltage speed of 10 kV.

X-ray diffraction (XRD; D8 Advance A25, Bruker, Karlsruhe, Germany) was used to determine activated carbon crystallinity, inter-crystal distance, and crystal size. XRD was operated with copper anode X-ray tube at 40 kV and 30 mA. The monochromatic radiation wavelength was 0.154 nm. The sample holder dimension was 25 mm × 1 mm. Scanning area at diffraction angle (2θ) was set at 0° to 50°. Other operation conditions included: scanning speed, 2°/min; interval, 0.02°; and divergence and scatter slit, 1° (Cheetam and Tao 1998). Relative crystallinity percentage is defined as crystalline component peak area ratio and is measured quantitatively. D-spacing and crystal size was

measured using the Bragg equation (Eq. 1) and peak width at half height of peak diffraction using the Scherrer equation (Eq. 2; Kim *et al.* 2010),

$$n\lambda = 2d \sin\theta \quad (1)$$

$$L = \frac{0.89\lambda}{\beta \cos\theta} \quad (2)$$

where n is an integer, λ is wavelength of the X-ray used, d is distance between crystal, θ is diffraction angle, L is crystal size, and β is peak width at half maximum (FWHM).

The activated carbon IR spectrum was measured by Fourier Transform Infrared Spectroscopy-Universal Attenuated Total Reflectance (FTIR-UATR/Perkin Elmer Spectrum Two C106456, Waltham, MA, USA). The samples were observed in transmission mode at wavelengths of 4000 to 400 cm^{-1}.

RESULTS AND DISCUSSION

Size Reduction of Activated Carbon Using High Energy Ball-mill

Milling for 150 min resulted in activated carbon particles with an average size of 449 nm. The result was not different from the milling in 180 min with a particle size of 448 nm, but it was different with milling for 80 min with a particle size of 1493 nm. For subsequent experiments, the activated carbon prepared by milling for 150 min was used. The PDI score was 0.66. This value indicates the particle size average distribution. If the PDI is lower than 0.7, then the sample particle size is judged to be adequately homogenous (Bera 2015; Sarmah *et al.* 2020).

The ball-milling treatment successfully reduced the size of the activated carbon to less than 500 nm. However, it was not successful in reducing the size below 100 nm. This finding is supported by Shan *et al*. (2016), where ball-milling at 550 rpm for 2 h for coconut shell-based activated carbon resulted in activated carbon with a size of 0.2 µm. Shan *et al.* (2016) showed that after 2 h, the activated carbon particle size was relatively constant with longer milling time. Wang *et al.* (2018) used ball-milling at 300 rpm for 12 h for bamboo-based activated carbon size reduction and produced activated carbon that was 525 to 253 nm. Lyu *et al.* (2018) used ball-milling at 300 rpm for 12 h for bamboo-based activated carbon size reduction and produced activated carbon of 33 to 333 nm.

Characteristics of Bamboo Charcoal and Bamboo Activated Carbon

This study characterized bamboo charcoal and bamboo activated carbon. Charcoal is a carbon-rich solid that is derived from organic materials heated in a limited oxygen environment (Strom 2020). Activated carbon is derived from biomass or other carbonaceous substances using pyrolysis (Strom 2020). In this study, carbon materials were activated physically and chemically. Table 1 indicates that bamboo charcoal produced a yield of 32.5% and burn-off weight percentage of 48.6. Activated carbon yield is determined by time, activation temperature, and type of raw material. Increasing the temperature and activation time decreases the activated carbon yield. Burn-off as an indicator of activation level is one of the crucial factors that determines the quality of activated carbon (Lazaro *et al.* 2007).

Table 1. Characteristics of Bamboo and Bamboo Charcoal

Parameters	Value
Water content of Bamboo (%)	17.02 ± 4.24
Water content of Bamboo charcoal (%)	3.64 ± 0.42
Yield of Bamboo charcoal (%)	32.54 ± 0.78
Burn off weight percentage (%)	48.55 ± 10.84

Several essential parameters for activated carbon are water content, ash content, and volatile matter content, as displayed in Table 2. All activated carbon met the criteria of the ANSI/AWWA B604-12 (2012) standard for moisture content, and most activated carbon met the criteria for ash content except for the activated carbon treated with $KMnO_4$.

The water content is influenced by the activating agent used, concentration of activating agent, and activated carbon particle size. The activating agent $KMnO_4$ produced a lower water content than KOH. KOH possesses a higher water absorbent capacity, so that the KOH in activated carbon can adsorb more water in the air. The higher concentration of activating agent produces activated carbon with lower water content. Ash content is affected by the type of material, type of activating agent, and concentration of activating agent. The activated carbon prepared with KOH contained a lower ash content. Volatile matter content is determined by the type of activating agent. The activating agent $KMnO_4$ produced activated carbon with lower volatile matter content than that of activating agent KOH.

Table 2. Water Content, Ash Content, and Volatile Matter of Bamboo Charcoal and Bamboo Activated Carbon

Sample	Moisture Content (%)	Ash Content (%)	Volatile Matter (%)
Bamboo charcoal	3.64	6.10	31.71
Phys. Activation	6.19	5.73	20.22
Act.KOH2.5%	6.67	4.82	18.04
Act. KOH2.5% &milling	7.18	4.23	20.69
Act.KOH5%	5.31	4.52	21.87
Act. KOH5% &milling	5.04	4.38	15.07
Act. $KMnO_4$ 2.5%	4.66	9.61	16.88
Act. $KMnO_4$ 2.5% &milling	4.45	9.89	18.22
Act. $KMnO_4$ 5%	4.65	14.49	15.94
Act. $KMnO_4$ 5% &milling	3.88	8.94	15.25
ANSI/AWWA B604-12 (2012)	Max 8	Max 6	na

Figure 1 depicts the fragments in the pyrolysates as determined by Py-GC/MS. The fragments of raw bamboo consist of 30 chemical component such as guaiacol, furfuryl alcohol, acetic acid, dimethyl phenol, dimethoxy phenol, acetosyringon, palmitic acid, propionic acid, propanon, benzofuran, and levoglucosan, as shown in Fig. 1a. After carbonization at 400 °C, the charcoal surface was dominated by long chain fatty acids such as stearic acid and lauric acid and aromatic compounds such as benzyl alcohol, syringol, and phenyl acetat (Fig. 1b). This result corresponds to the high content of volatile matter and carbon content in bamboo charcoal (Table 2).

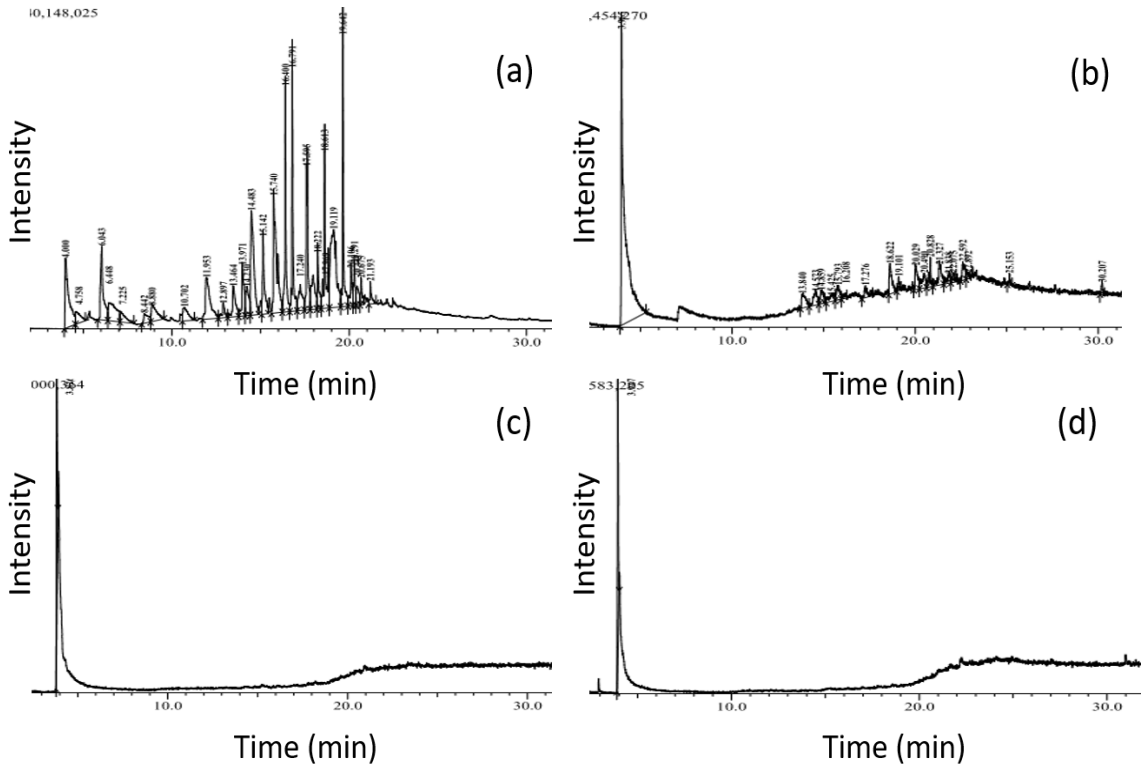

Fig. 1. Chromatogram of (a) bamboo, (b) bamboo charcoal, (c) bamboo activated KOH & milling, and 194 (d) bamboo activated $KMnO_4$ & milling

After further carbonization and activation at 800 °C, the acid content in carbon activated with KOH and $KMNO_4$ increased. The compound attached to the surface of activated carbon was ammonium carbamate (Fig. 1c and 1d). This result showed that all lignocellulosic compounds such as lignin, cellulose, and hemicellulose were converted to carbon atoms. The low volatile matter and high carbon content (Table 2) supported the results of the XRD (Fig. 5) and FTIR analyses (Fig. 4), which show the arrangement of carbon atoms. The C content increased after activation, while the contents of O and N decreased notably, implying the elimination of those groups during the activation process. This was consistent with research conducted by Liu *et al*. (2010).

The pyrolysis process at high temperature to activate bamboo charcoal affected the volatile fragments. The increasing heating rate broke chemical bonds, and the volatile products were removed by the carrier gas. This phenomenon shows that the lignocellulose compound in bamboo such as cellulose, lignin and hemicellulose was decomposed into carbon.

Iodine Number and Methylene Blue Adsorption

Figure 2 presents the iodine number of charcoal and activated carbon (a) and adsorption level of methylene blue (b). According to ANSI/AWWA B604-12 (2012), the minimum iodine number was 500 mg/g. Methylene blue adsorption according to JIS K 1474 (1967) was 180 to 230 mg/g.

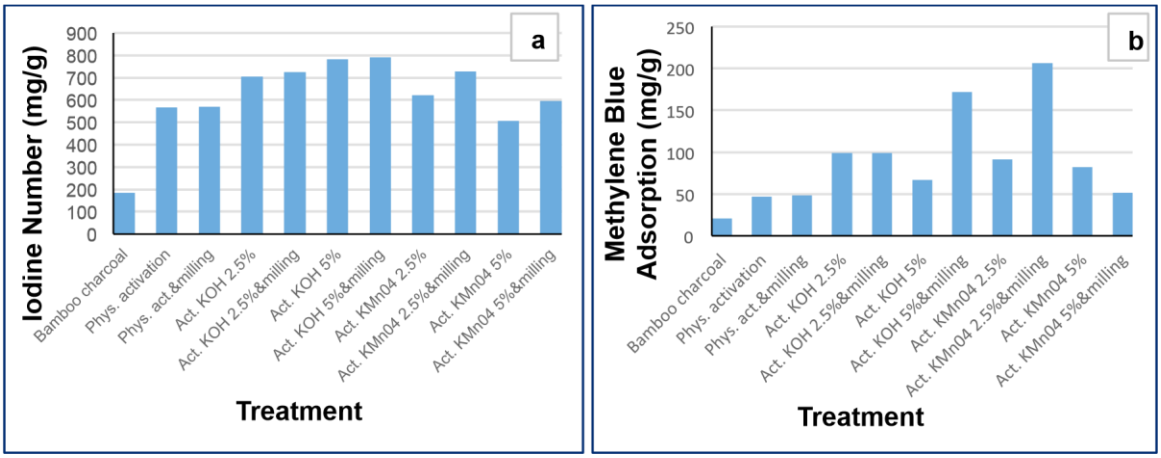

Fig. 2. Iodine number (a) and methylene blue adsorption (b) of activated carbon

The activated carbon that met the criteria for iodine number and had the highest iodine number was milled activated carbon treated with activating agent KOH 5% (790 mg/g). This result was higher than that of reported by the following researchers. Santana *et al*. (2019) reported that iodine number of bamboo activated carbon with activating agent H_3PO_4/H_2 was 748 mg/g. Huang *et al.* (2014) reported that iodine number of bamboo activated carbon with activating agent Nitrogen gas and carbonization temperature of 1000 °C was 78.6 mg/g. Meanwhile, Mahanim *et al*. (2011) reported that iodine number of bamboo activated using stem at 800 °C was 823 mg/g. Carbon biomass with iodine number between 600 and 1450 mg/g is considered activated carbon (ASTM 2011). This indicates the development of pores structures. Meanwhile, iodine number indicated a huge number of micro pores (the small size pores with size less than 2 nm). Activated carbon with micropores have adsorption capacity for smaller substances (ASTM 234 D 4607-94 1994). Haimour and Emeish (2006) stated that the iodine number indicates the number of pores with size larger than 1.0 nm. Mahanim *et al.* (2011) studied the effect of activation temperature on iodine number at different activation times. The iodine number increased with increasing the activation temperature. When the activation temperature increased above 800 °C, the particles were burned out completely due to very high gasification rates. When the activating agent comes in contact with the char, it reacts both with the exterior and interior of the particle, in which most of the disorganised carbon is removed (Kumar *et al.* 2006).

Activated carbon specimens that met criteria for iodine number and methylene blue adsorption were milled activated carbon with activating agent $KMnO_4$ 2.5%, with methylene blue adsorption 206 mg/g. This result was lower than that of reported by other researchers. Hameed *et al.* (2007) reported that methylene blue adsorption of bamboo activated carbon with activating agent KOH/CO_2 was 454 mg/g, whereas Santana *et al.* (2019) reported that methylene blue adsorption of bamboo activated carbon with activating agent CO_2 was 299 mg/g. Meanwhile, Liu *et al*. (2010) reported that methylene blue adsorption of bamboo activated carbon with activating agent phosphoric acid was 320 mg/g.

The enhanced adsorption of methylene blue on the activated carbon should be attributed primarily to the enlargement of the micropores, which made more sites accessible for methylene blue. According to the study of Pelekani and Snoeyink (2000), effective adsorption of methylene blue (with molecular dimensions of 1.43 nm × 0.61 nm

× 0.4 nm) occurred within pores with a width above 0.75 nm. Enhanced adsorption of methylene blue benefited from the addition of mesopores has also been reported by Lei *et al*. (2006).

The methylene blue adsorption test was conducted to measure the material ability to adsorb colours and substance with large molecules connected to mesopores and macropores (Raposo *et al*. 2009), even though it is also found in micropores in small amounts. Compared with methylene blue, iodine molecules have smaller dimensions which makes it easier for them to penetrate micro pores. The hydrothermal process at low temperature produces less micro pores than mesopores and macro pores.

All milling treatment exhibited better methylene blue adsorption except for $KMnO_4$ 5% & milling, which had lower adsorption than Act. KMnO4 5%. This was presumably because 5% concentration of $KMnO_4$ exceeded the optimum concentration. Li *et al*. (2017) stated that pore volume increases rapidly with the impregnation ratio increasing. This is because higher impregnation ratio causes higher activation degrees, so more pores will be generated and pore volume will be enlarged. Nevertheless, when the impregnation ratio exceeds the optimal concentration, the situation turns to the opposite. If the mass ratio exceeds the optimal concentration not only the carbon atoms on the active sites will be consumed completely, but also the carbon atoms on lattice surface will be consumed. In that way, some micropores will be ablated exceedingly, and pore volume in the micropore range will decrease. Ball milling treatment could be worsen the condition of the ablated pores.

The milling process gave rise to activated carbon with higher iodine number and methylene blue adsorption compared to non-milling activated carbon. The ball milling process also decreased the activated carbon crystallinity, which indicates that the material was amorphous. The Ilkovic equation is commonly used for describing diffusion-controlled kinetics of irreversible adsorption of proteins at solid/liquid interfaces (Hibbert *et al*. 2002; Miyazaki *et al*. 2017). This model assumes that the molecules that come into contact with the adsorbent surface are rapidly adsorbed, thus generating a concentration gradient between the bulk solution and the solution close to the surface.

Diffusion kinetics, which largely depends on the crystal structure of carbon and the enhanced diffusivity in milled bamboo activated carbon, can be manipulated by increasing partial graphitization within amorphous carbon, as confirmed by XRD and FTIR analyses. An increasing in mesoporosity of milled activated carbon, as observed from BET analysis, can also positively affect diffusion kinetics by decreasing the charge transfer resistance. In addition, ball-milling activated carbon can control its physical properties, such as crystallinity and porosity. The milled activated carbon with increased graphitization and well develop meso-porosity via both diffusion-controlled transport and surface-limited adsorption/desorption.

Surface Area Analysis (BET)

Surface area indicates the adsorption capacity of adsorbent or porous materials. Activated carbon covers a surface area of 300 to 4000 m^2/g and is the largest of all adsorbents (Yang *et al*. 2002).

Activated carbon size reduction is expected to increase the specific surface area and pore total volume. Table 3 presents the BET surface area analysis of activated carbon. The average surface area and activated carbon pore volume after ball-milling increased, but the average pore radius decreased. KOH treatment resulted in relatively larger surface area

compared with treatment with $KMnO_4$. The pore radius of the sample activated using $KMnO_4$ was larger than that of the sample activated using KOH.

Table 3. Surface Area Analysis (BET) of Bamboo Charcoal and Bamboo Activated Carbon

Sample	Surface Area (m^2/g)	Pore Volume (cc/g)	Pore Radius (nm)
Bamboo charcoal	24.29	0.02	9.46
Physical activation	293.26	0.01	1.70
Act. KOH2.5%	467.57	0.29	1.18
Act. KOH2.5%&milling	549.36	0.23	2.21
Act. KOH5%	516.05	0.27	2.19
Act. KOH5%&milling	554.53	0.28	1.20
Act. $KMnO_4$ 2.5%	412.62	0.18	2.45
Act. $KMnO_4$ 2.5%&milling	516.52	0.23	2.30
Act. $KMnO_4$ 5%	405.84	0.33	2.49
Act. $KMnO_4$ 5%&milling	445.87	0.82	2.25

The study produced activated carbon with pore radius ranging from 1.18 nm to 2.49 nm. Bamboo charcoal before activation had a pore radius larger than 9 nm. This showed that activation treatment and milling produced activated carbon with smaller pore size. Table 3 shows that activated carbon with the highest surface area was the Act. KOH 5% and milling. The activated carbon with largest nano size pore volume was the Act.$KMnO_4$ 5% and milling.

The ball-milling treatment altered the ratio physisorbed gas to chemisorbed gas, and this finding is in accordance with previous research (Welham *et al.* 2002; Abdul Khalil *et al.* 2013). The longer the milling time caused agglomeration to occur from smaller particles into larger particles. The pore size of the activated carbon ranged from 2 to 50 nm, which is categorised as mesopore structure.

Based on the results of nitrogen adsorption as shown in BET analysis, micropores (pores smaller than 2 nm) were dominant. The type of pore formed from the milling process using ball milling is mesopore, the smaller the particle size produced, the more pores that are formed and the greater the absorption capacity (Hu *et al.* 2019). The type of pore that was increased due to the ball-milling process was mesopore. When smaller particles are produced, there are more pores formed, resulting in higher adsorption.

Because of the catalytic effect of potassium, tar can be further cracked, while char is gasified into the gases. Many new pores are formed rapidly (Wang and Kaskel 2012). KOH is alkaline with lower ionisation energy when dissolved in water. Lower ionization energy indicates a weaker strength of the ionic bond between a metal atom (*i.e.* K) and hydroxyl ion (OH-), thus the bond can be easily broken when dissolved in water to form an aqueous solution. The result is release of more hydroxyl (OH-) ions in the aqueous solution of KOH. These hydroxyl ions were likely to have attacked and weakened the chemical bonds present within the char matrix (*e.g.* the covalent bond between the monomer units such as ether bond (–C–O–C–) of lignocellulosic components) during the chemical impregnation step.

KOH is a powerful reagent because it can interact with carbon atoms and serves as a catalyst for dehydrogenase reaction and oxidation, therefore increasing porosity (Abdul

Khalil *et al*. 2013). Girgis and El-Hendawy (2002) showed that the amount of KOH affects the activated carbon produced. Girgis and El-Hendawy (2002) used KOH with the raw material to KOH ratio of 1:3. The higher ratio of KOH can cause the formation of an insulation layer and encapsulate particles, thus reducing the activation process and contact with the surrounding environment (Girgis and El-Hendawy 2002).

Morphology Analysis (SEM)

SEM images of the charcoal and activated carbon (Fig. 3) showed the size of the activated carbon pore. There were a number of nano-size pores (mesopore and micropore, which are too small to be seen distinctly in the micrographs), along with some particles larger than 1 µm. Activation treatment produced more pores compared with carbon with pyrolysis treatment without activation. The milling process using ball-milling reduced the size of particles. The process also produced smaller activated carbon with increased surface area. However the reduced particle size can also cause some small particles to cover macropores and mesopores. According to Abdul Khalil *et al.* (2013) and Welham *et al.* (2002), ball-milling changes the ratio of physisorbed gas to be chemisorbed gas.

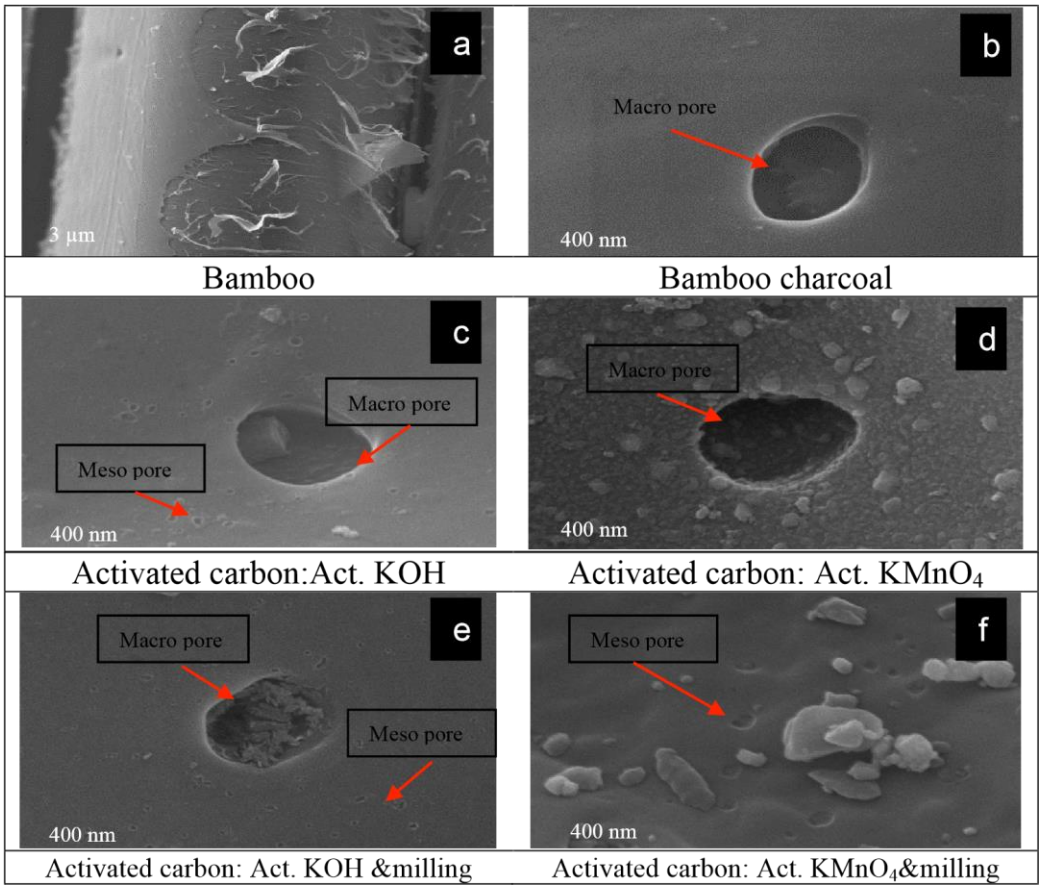

Fig. 3. SEM image of bamboo (a), bamboo charcoal (b), bamboo activated carbon (c, d, e, f) taken at approximately 5000x and 50000x magnification

The activating agent KOH produced activated carbon with finer surface, while $KMnO_4$ produced a rough surface. The blocking of pores by smaller particles occurred more often with activating agent $KMnO_4$. Microstructure images showed that the number

of pores increased due to carbonation and activation, but it was difficult to compare it accurately (Negara *et al.* 2019). Ball-milling reduced the size of activated carbon particles.

Functional Group Analysis (FTIR)

The FTIR test was conducted to identify the functional group of activated carbon. Increases and decreases in spectral peaks indicate the impact of treatment to the material structure, as presented in Fig. 4. The C=O bond and C-O stretching at wave number 1640 to 1750 cm^{-1} is attributed to phenolic ester and ketone. Peaks in the range of wavenumbers 700 to 900 cm^{-1} are related to aromatics (Cuhadaroglu and Uygun 2008).

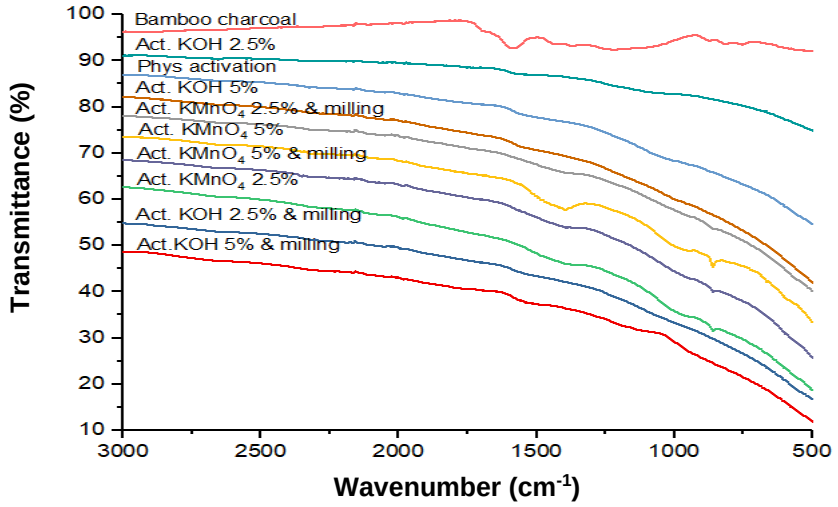

Fig. 4. FTIR spectra of bamboo charcoal and bamboo activated carbon

The peak at wave number 1600 to 1400 cm^{-1} showed the aromatic C=C bond from lignin. In this wave number range are benzene (1450 cm^{-1}), aromatic structures (1600 cm^{-1}), and methoxyl groups (1470 to 1430 cm^{-1}) (Gao *et al.* 2011). The OC-O bond (carboxyl) at wave number 1250 to 1000 cm^{-1} had a higher peak, which decreased after the hydrothermal process (Cuhadaroglu and Uygun 2008).

Absorbance at wave number 500 to 800 cm^{-1} was connected to aromatic substitution. Cellulose was indicated by strong absorption on –OH and C–O, while hemicellulose was indicated by the presence of C=O (aldehyde) (Yang *et al.* 2007). Lignin spectrum at 1428 cm^{-1} is the stretching vibration of $–CH_3O$ (Huang *et al.* 2015). The result of the FTIR analysis showed that lignin content was still high and only fractionally reduced, while cellulose and hemicellulose content was very limited. This finding was in accordance with the research finding of Sumtong *et al.* (2017), which stated that lignin content was only slightly decomposed while cellulose and hemicellulose were almost entirely decomposed in hydrothermal process.

Figure 4 illustrates the comparison of carbon FTIR spectrum before and after activation and size reduction. Carbon has C=C bond (wave number 1631 cm^{-1}), but it did not emerge after activation. The new peak of the active carbon occurred at wave number 1573 cm^{-1}, which showed the stretching of C-C because of the newly formed aromatic ring. This reinforced the fact that the activated carbon was formed because of the new pore formation (Muniandy *et al.* 2014; Thuan *et al.* 2016). The activation process also broke many chains either aliphatic or aromatic (Hesas *et al.* 2013). This effect was shown by the

decrease in transmittance at the area of 1195 to 459 cm^{-1}. The peak at 1195 cm^{-1} indicated C-O stretching.

Analysis of Crystallinity (XRD)

Figure 5 shows the XRD results of bamboo-based activated carbon. The peak of XRD spectrum on raw material appeared sharp, clear, and higher than the spectral peak of activated carbon. Diffractograms at 16° and 23º indicated an A-type starch diffraction pattern (Jiang *et al.* 2010). The entire solid showed a broadening peak at the area of 20 to 30º, which is characteristic of carbon. Diffraction peaks at 23.4º and 43.7º indicated amorphous carbon. Some researchers stated that activated carbon is amorphous material (Ip *et al*. 2008; Jung *et al*. 2011; Mohamed *et al*. 2017).

The peak intensity at 23° decreased. This indicated that cellulose decomposed into elemental carbon after the activation process. The broadening peak at 23.4° in carbon material indicated that atom bond gradually disappeared and established the hexagonal structures. Activation process causes inter-aromatic layers that are not symmetrical so that the degree of crystallinity decreased.

Activation using KOH involves carbon gasification and potassium metal intercalation, which quickly disappears (Marsh and Rodríguez-Reinoso 2006). Gasification on the carbon surface causes macropore formation.

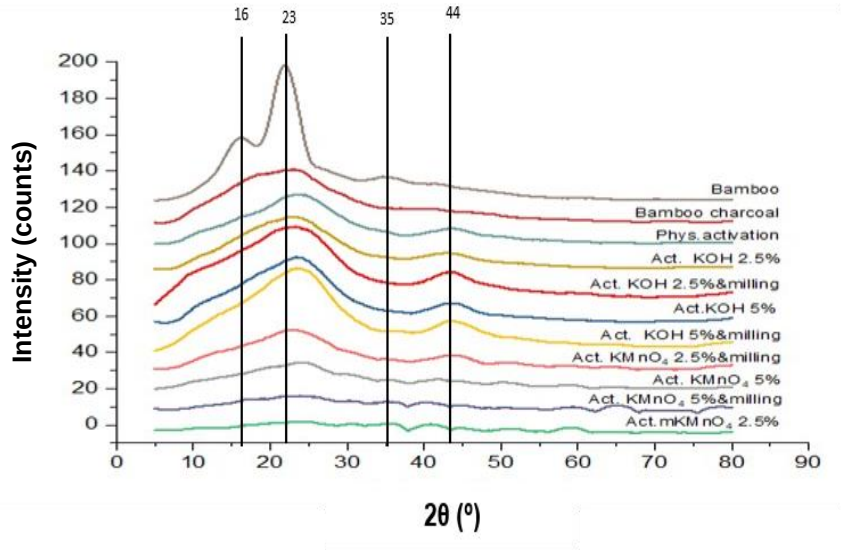

Fig. 5. XRD analysis of bamboo activated carbon

Ball-milling treatment produced smaller active carbon particles, as shown by broad peak area, which was connected to the weakening of reflection intensity of the plane (002). It was assumed that the original crystal structure had been modified by the ball milling treatment (Zhang *et al*. 2019). The broad peak at 22 to 23° is related to the plane reflection (002) from carbon (Qu 2002; Bratek *et al.* 2013). This broad peak showed that activated carbon is not crystalline (Welham and Williams 1998). The peak at 43 to 44° narrowed with low intensity. This peak is related to the plane reflection (100) (Zhang *et al.* 2019).

Table 4 shows that activated carbon with activating agent KOH had lower crystallinity compared with the one with $KMnO_4$ activating agent. Surface area in the case of KOH activated carbon is higher than KMnO4 because the dispersion of particle is better

in case of KOH activated carbon. KOH was found to be more effective than potassium permanganate in creating porosity in activated carbons.

According to Wu *et al.* 2019, the loading of potassium permanganate onto the activated carbon did not change the lattice structure of the carbon. The higher crystallinity on activated carbon with $KMnO_4$ was because the distance of aromatic structure (d) decreased along with narrowing the width of aromatic structure. This changing resulted in a low level of regularity structure (amorphous) becoming regular (crystalline). This is in accordance with Stevens' (2007) statement that the tendency for the formation of crystallinity increases with the increasing of stereo regularity. This regularity occurs because there is shifting in the crystalline structure of activated carbon (Schukin *et al.* 2002). This study proves that activated carbon with $KMnO_4$ will produce the greater crystallinity.

The ball-milling treatment also decreased the degree of crystallinity of activated carbon, which means that activated carbon was amorphous. Pore structure was formed during the carbonation and activation process when the distance between basic crystals is cleared from tar and other elements (Bansal and Goyal 2005).

Table 4. Crystallite Size and Crystallinity of Bamboo-based Activated Carbon

Material	d-Spacing (nm)			Crystallite Size (nm)			Crystallinity
	Peak 1	Peak 2	Peak 3	Peak 1	Peak 2	Peak 3	(%)
Raw Bamboo	0.40	0.42	0.43	3.649	7.431	7.216	23.5614
Bamboo charcoal	0.48	0.6	0.40	167.85	162.285	57.886	16.0693
Physical activation	0.41	0.38	0.37	40.459	81.221	46.919	23.3912
Act. KOH 2.5%	0.38	0.41	0.40	58.004	53.972	101.295	13.7961
Act. KOH 2.5%+mill	0.41	0.40	0.38	67.482	115.778	81.171	8.1175
Act. KOH 5%	0.77	0.21	0.42	38.050	50.391	48.535	14.3354
Act. KOH 5%+mill	0.41	0.39	0.38	21.303	36.875	20.300	10.6417
Act. $KMnO_4$ 2.5%	0.22	0.26	0.29	23.556	52.110	41.287	48.3738
Act. $KMnO_4$ 2.5%+mill	0.37	0.29	0.36	67.763	32.588	81.419	31.2841
Act.$KMnO_4$ 5%	0.12	0.29	0.39	28.465	68.801	45.058	18.5378
Act. $KMnO_4$ 5%+mill	0.12	0.14	0.23	28.101	87.732	55.834	21.1896

CONCLUSIONS

1. The study produced nanopore activated carbon with a size of 449 nm and PDI score of 0.66 using ball-milling treatment for 150 min. The pore radius of the activated carbon was in the range 1.18 to 2.49 nm.
2. Ball-milling treatment increased the activated carbon surface area and pore volume, but it decreased the crystallinity. The milled activated carbon will develop meso-porosity *via* both diffusion-controlled transport and surface-limited adsorption/desorption.
3. The activated carbon which met the criteria of the ANSI/AWWA B604-12 (2012) standard for moisture content, iodine number, and the JIS K 1474 (1967) standard 393 for methylene blue adsorption level and surface area were milled activated carbon with activator $KMnO_4$ 2.5%.

4. This study demonstrated that ball-milling activated carbon with activator $KMnO_4$ was a promising carbon material for usage as an adsorber.

ACKNOWLEDGEMENTS

The financial support from Indonesian Agency for Agricultural Research and Development, Ministry of Agriculture is highly appreciated.

REFFERENCES CITED

Abdul Khalil, H. P. S., Jawaid, M., Firoozian, P., Rashid, U., Islam. A., and Akil, H.M. (2013). "Activated carbon from various agricultural wastes by chemical activation with KOH: Preparation and characterization," *J. Biobased. Mater.* 7, 1-7. DOI: 10.1166/jbmb.2013.1379

Ahmed, M. J., and Theydan, S. K. (2012). "Adsorption of cephalexin onto activated carbons from *Albizia lebbeck* seed pods by microwave-induced KOH and K_2CO_3 activations," *Chem. Eng. J.* 211–212, 200-207. DOI: 10.1016/ j.cej.2012.09.089

American Society for Testing and Materials (ASTM D 4607-94). (1994). "Standard test method for determination of iodine number of activated carbon (Reapproved 2006)," ASTM International, West Conshohocken, USA.

American Society for Testing and Materials (ASTM D4607-9)4. (2011). "Standard test method for determination of iodine number of activated carbon," ASTM International, West Conshohocken

ANSI/AWWA B604-12 (2012). "Standard for granular activated carbon," American Water Works Association, Denver, CO, USA.

Aygun, A., Yenisoy-Karaka, S., and Duman, I. (2003). "Production of granular activated carbon from fruit stones and nut shell sand evaluation of their physical, chemical and adsorption properties," *Micropor. Mesopor. Mat.* 66(2-3), 189-195. DOI: 10.1016/j.micromeso.2003.08.028

Bansal, R. C., and Goyal, M. (2005). *Activated Carbon Adsorption*, CRC Press, Boca Raton, FL, USA.

Bera, A. (2015). "Nanoporous silicon prepared by vapour phase strain etch and sacrificial technique," in: *Proceedings of the International Conference on Microelectronic Circuit and System (Micro)*, Kolkata, India, pp. 42-45, (https://pdfs.semanticscholar.org/90d7/5357faa004f0cf15abf2ad458f8e1253f15d.pdf).

Boudrahem, F., Soualah, A., and Aissani-Benissad, F. (2011). "Pb (II) and Cd (II) removal from mechanochemical treatment can reduce particle sizes and activate their surface chemical states, aqueous solutions using activated carbon developed from coffee residue activated with phosphoric acid and zinc chloride," *J. Chem. Eng. Data.* 56 (5), 1946-1955. DOI: 10.1021/je1009569

Bratek, W., Świą tkowski, A., Pakuła, M., Biniak, S., Bystrzejewski, and Szmigielski, R. (2013). "Characteristics of activated carbon prepared from waste PET by carbon dioxide activation," *J. Anal. Appl. Pyrol.* 100, 192–198. DOI: 10.1016/j.jaap.2012.12.021

Cheetam, N. W. H. and Tao, L. (1998). "Variation in crystalline type with amylose content in maize starch granules: An x-ray powder diffraction study," *Carbohydr. Polym.* 36, 277-284. DOI: 10.1016/S0144-861(98)00007-1

Chen, Z., Zhang, H., He, Z., Zhang, L., and Yue, X. (2019). "Bamboo as an emerging resources for worldwide pulping and papermaking," *BioResources* 14(1), 3-5. DOI: 10.15376/biores.14.1.3-5

Chmiola, J., Largeot, C., Taberna, P. L., Simon, P., and Gogotsi, Y. (2008). "Desolvation of ions in subnanometer pores and its effect on capacitance and double-layer theory," *Angew. Chem.* 120(18), 3440-3443. DOI: 10.1002/anie.200704894

Cuhadaroglu and Uygun. (2008). "Production and characterization of activated carbon from bituminous coal by chemical activation," *Afr. J. Biotechnol*. 7(20), 3703-3710. DOI: 10.5897/AJB08.588

Deiana, C., Granados, D., Venturini, R., Amaya, A., Sergio, M., and Tancredi, N. (2008). "Activated carbons obtained from rice husk: Influence of leaching on textural parameters," *Ind. Eng. Chem. Res.* 47(14), 4754-4757. DOI: 10.1021/ie071657x

Gao, Y., Chen, H. P., Wang, J., Shi, T., Yang, H. P., and Wang, X. H. (2011). "Characterization of products from hydrothermal liquefaction and carbonation of biomass model compounds and real biomass," *J. Fuel. Chem. Technol.* 39(12), 893-900. DOI: 10.1016/s1872-5813(12) 60001-2

Frimmel, F. H., Abbt-Braun, G., Heumann, K. G., Hock, B., Lüdemann, H.-D., and Spiteller, M. (2002). *Refractory Organic Substances in the Environment*, Wiley-VCH, Weinheim.

Galhena, D. T. L., Bayer, B.C., Hofmann, S., and Amaratunga, G. A. J. (2016). "Understanding capacitance variation in sub-nanometer pores by in situ tuning of interlayer constrictions," *ACS. Nano.* 10(1), 747-754. DOI: 10.1021/acsnano.5b05819

Garcia-Garcia, A., Gregorio, A., Boavida, D., and Gulyurtlu, I. (2002). "Production and characterization of activated carbon from pine wastes gasified in a pilot reactor," *National Institute of Engineering and Industrial Technology, Edif. J.*, Estrada do Paco do Lumiar, 22, 1649-038, Lisbon, Portugal

Giraldo, L., and Moreno-Piraján J. C. (2008). "Pb^{2+} adsorption from aqueous solutions on activated carbons obtained from lignocellulosic residues," *Braz. J. Chem. Eng.* [online]. 25(1), 143-151. DOI: 10.1590/S0104-66322008000100015**.**

Girgis, B. S, and El-Hendawy, A. N. A. (2002). "Porosity development in activated carbons obtained from date pits under chemical activation with phosphoric acid," *Micropor. Mesopor. Mat*, Vol. 52, Issue 2, April 2002, Pages 105-117. DOI: 10.1016/S1387-1811(01)00481-4

Gonçalves, M., Sánchez-García, L., Oliveira-Jardim, E., Silvestre-Albero, J., and Rodríguez-Reinoso, F. (2011). "Ammonia removal using activated carbons: Effect of the surface chemistry in dry and moist conditions," *Environmental Science & Technology*. 45(24), 10605-10610. DOI: 10.1021/es203093v

Haimour, N. M., and Emeish, S. (2006). "Utilization of date stones for production of activated carbon using phosphoric acid," *Waste. Manag.* 26, 651-660. DOI: 10.1016/j.wasman.2005.08.004

Helland, A., Wick, P., Koehler, A., Schmid, K., Som, C. (2007). "Reviewing the environmental and human health knowledge base of carbon nanotubes," *Environmental Health Perspectives* 115, 1125-1131.

Hameed, B. H., Din, A. T. M., Ahmad, A. L. (2007). "Adsorption of methylene blue onto bamboo-based activated carbon: Kinetics and equilibrium studies," *Journal of Hazardous Materials* 141, 819-825.

Hesas, R., Niya, H., Daud, A., and Sahu, W. J. N. (2013). "Preparation and characterization of carbon from apple waste by microwave-assisted phosphoric acid activation: Application in methylene blue," *BioResources* 8(2), 2950-2966. DOI: 10.15376/biores.8.2.2950-2966

Hibbert, D. B., Gooding, J. J., and Erokhin, P. (2002). "Kinetics of irreversible adsorption with diffusion: Application to biomolecule immobilization," *Langmuir* 18, 1770-1776. DOI: 10.1021/la015567n

Hu, S., Zhang, D., Yang, Y., Ran, Y., Mao, J., Chu, W., and Cao, X. (2019). "Effects of the chemical structure, surface, and micropore properties of activated and oxidized black carbon on the sorption and desorption of phenanthrene," *Environ. Sci. Technol.* 53, 7683-7693. DOI: 10.1021/acs.est.9b01788

Huang, P. H., Jhan, J. W., Cheng, Y. M., and Cheng, H. H. (2014). "Effects of carbonization parameters of moso-bamboo-based porous charcoal on capturing carbon dioxide," *Scientific World Journal* 2014, article ID 937867, 8 pages. DOI: 10.1155/2014/937867

Huang, Y. X., Ma, E., and Zhao, G. J. (2015). "Thermal and structure analysis on reaction mechanisms during the preparation of activated carbon fibers by KOH activation from liquefied wood-based fibers," *Ind. Crop. Prod.* 69, 447-455. DOI: 10.1016/j.indcrop.2015.03.002

Ip, A. W. M., Barford, J. P., and McKay, G. (2008). "Production and comparison of high surface area bamboo derived active carbons," *Bioresource Technol.* 99(18), 8909-8916. DOI: 10.1016/j.biortech.2008.04.076

Jiang, R., Zhu, H. Y., Zeng, G. M, Xiao, L., and Guan, Y. J. (2010). "Synergy of adsorption and visible light photo catalysis to decolor methyl orange by activated carbon/nanosized CdS/chitosan composite," *J. Cent. South Univ. Technol.* 17, 1223-1229 (2010). DOI: 10.1007/s11771-010-0623-0

Jung, M. J., Jeong, E., Kim, S., Lee, S. I., Yoo, J. S., and Lee, Y. S. (2011). "Fluorination effect of activated carbon electrodes on the electrochemical performance of electric double layer capacitors," *J. Fluor Chem.* 132(12), 1127-1133. DOI: 10.1016/j.jfluchem.2011.06.046

Kant, P. (2010). "Should bamboos and palms be included in CDM forestry projects?" IGREC Working paper No. IGREC- 07: 2010, Institute of Green Economy, New Delhi, India.

Kazmierczak, J., Nowicki, P**.,** and Pietrzak, R. (2013). "Sorption properties of activated carbons obtained from corn cobs by chemical and physical activation," *Adsorption* 19, 273-281. DOI: 10.1007/s10450-012-9450-y

Kim, S. H., Shon, H. K., and Ngo, H. H. (2010). "Adsorption characteristics of antibiotics trimethoprim on powdered and granular activated carbon," *J. Ind. Eng. Chem.* 16(2010), 344-349. DOI: 10.1016/j.jiec.2009.09.061

Kumar, P. B. G., Shivakamy, K., Miranda, L. R., and Velan, M. (2006). "Preparation of steam activated carbon from rubberwood sawdust (*Hevea brasiliensis*) and its adsorption kinetics," *Journal of Hazardous Materials B* 136, 922-929.

Lam, C. W., James, J. T., McCluskey, R., Arepalli, S., and Hunter, R. L. (2006). "A review of carbon nanotube toxicity and assessment of potential occupational and

environmental health risks," C*ritical Reviews in Toxicology* 36(3), 189-217. DOI: 10.1080/10408440600570233

Lázaro, M. J., Gálvez, M. E., Artal, S., Palacios, J. M., and Moliner, R. (2007). "Preparation of steam-activated carbons as catalyst supports," *J. Anal. Appl. Pyrolysis.* 78(2), 301-315. DOI: 10.1016/j.jaap.2006.08.007

Lei, S., Miyamoto, J., Kanoh, H., Nakahigashi, Y., and Kaneko, K. (2006). "Enhancement of the methylene blue adsorption rate for ultramicroporous carbon fiber by addition of mesopores," *Carbon* 44, 1884-1890.

Li, S., Han, K., Li, J., Li, M., and Lu, C. (2017). "Preparation and characterization of super activated carbon produced from gulfweed by KOH activation," *Microporous Mesoporous Mater*. 243, 291-300.

Liu, Q. S., Zheng, T., Wang, P., and Guo, L. (2010). "Preparation and characterization of activated carbon from bamboo by microwave-induced phosphoric acid activation," *Ind. Crop. Prod.* 31, 233-238. DOI: 10.1016/j.indcrop.2009.10.011

Liu, Q. S., Zheng, T., Li, N., Wang, P., and Abulikemu, G. (2010). "Modification of bamboo-based activated carbon using microwave radiation and its effects on the adsorption of methylene blue," *Applied Surface Science* 256, 3309-3315.

Liu, J. J., Deng, Y. F., Li, X. H., and Wang, L. F. (2016). "Promising nitrogen-rich porous carbons derived from one-step calcium chloride activation of biomass-based waste for high performance supercapacitors," *ACS Sustainable Chem. Eng.* 4(1), 177-187. DOI: 10.1021/acssuschemeng.5b00926

Lyu, H., Gao, B., He, F., Ding, C., Tang, J., and Crittenden, J. C. (2017). "Ball-milled carbon nanomaterials for energy and environmental applications," *ACS Sustain Chem. Eng.* 5, 9568-9585. DOI: 10.1021/acssuschemeng.7b02170

Lyu, H., Gao, B., He, F., Zimmerman, A. R., Ding, C., Huang, H., and Tang, J. (2018). "Effects of ball milling on the physicochemical and sorptive properties of biochar: Experimental observations and governing mechanisms," *Environ. Pollut.* 233, 54-63. DOI: 10.1016/j.envpol. 2017.10.037

Mahanim, S. M. A., Asma, I. W., Rafidah, J., Puad, E., and Shaharuddin, H. (2011). "Production of activated carbon from industrial bamboo wastes," *Journal of Tropical Forest Science* 23(4), 417-424.

Marsh, H., and Rodríguez-Reinoso, F. (2006). *Activated Carbon*, Elsevier, Amsterdam.

Miyazaki, C. M., Mishra, R., Kinahan, D. J, Ferreira, M., and Ducrée, J. (2017). "Polyethylene imine/grapheme oxide layer-by-layer surface functionalization for significantly improved limit of detection and binding kinetics of immunoassays on acrylate surfaces," *Colloids Surf B* 158, 167-174. DOI: 10.1016/j.colsurfb.2017. 06.042

Mohamed, M. A., Salleh, W. N. W., Jaafar, J., Rosmi, M. S., Mohd. Hir, Z. A., Mutalib M. A., Ismail, A. F., and Tanemura, M. (2017). "Carbon as amorphous shell and interstitial dopant in mesoporous rutile TiO_2: Bio-template assisted sol-gel synthesis and photocatalytic activity," *Appl. Surf.* 393(30), 46-59. DOI: 10.1016/j.apsusc.2016.09.145

Muniandy, L., Adam, F., Mohamed, A. R., and Ng, E. P. (2014). "The synthesis and characterization of high purity mixed microporous/mesoporous activated carbon from rice husk using chemical activation with NaOH and KOH," *Micropore. Mesopore. Mat.* 197, 316-323. DOI: 10.1016/j.micromeso.2014.06.020

Nagaraju, G., Lim, J. H., Cha, S. M., and Yu, J. S. (2016). "Three-dimensional activated porouscarbon with meso/macropore structures derived from fallen pine cone flowers: A low-cost counterelectrode material in dye-sensitized solar cells," *J. Alloys. Compd.* 693, 1297-1304. DOI: 10.1016/j.jallcom.2016.10.015

Negara, D. N. K. P., Nindhia, T. G. T., Surata, V., Sucipta, M., and Hidajat, F. (2019). "Activated carbon characteristics of tabah bamboo that physically activated under different activation time," *IOP Conf. Series: Materials Science and Engineering* 539 (2019) 012011. DOI: 10.1088/1757-899X/539/1/012011

Pang, M., Liu, B., Kano, N., and Imaizumi, H. (2015). "Adsorption of chromium (VI) onto activated carbon modified with $KMnO_4$," *J. Chem. Chem. Eng*. 9(2015), 280-287. DOI: 10.17265/1934-7375/2015.04.006

Pelekani, C., and Snoeyink, V. L. (2000). "Competitive adsorption between atrazine and methylene blue on activated carbon: The importance of pore size distribution," *Carbon.* 38, 1423-1436.

Peterson, S. C., Jackson, M. A., Kim, S., and Palmquist, D. E. (2012). "Increasing biochar surface area: Optimization of ball milling parameters," *Powder Technology* 228(Sept.), 115-120.

Qu, D. (2002). "Studies of the activated carbons used in double-layer super capacitors," *J. Power Sources* 109(2), 403-411. DOI: 10.1016/S0378-7753(02)00108-8

Raposo, F., Rubia, M. A. D. L., and Borja, R. (2009). "Methylene blue number as useful indicator to evaluate the adsorptive capacity of granular activated carbon in batch mode: influence of adsorbate/adsorbent mass ratio and particle size," *J. Hazard. Mater.* 165, 291-299. DOI: 10.1016/j.jhazmat.2008.09.106

Rathnayake, D. N., Korotta-Gamage, S. M., Kastl, G., and Sathasivan, A. (2017). "Effect of $KMnO_4$ treatment of granular activated carbon on the removal of natural organic matter," *Desalin. Water Treat.* 71, 201-206. DOI: 10.5004/dwt.2017.20570

Raymundo-Piñero, E., Kierzek, K., Machnikowski, J., and Béguin, F. (2006). "Relationship between the nanoporous texture of activated carbons and their capacitance properties in different electrolytes," *Carbon* 44 (12), 2498-2507. DOI: 10.1016/j.carbon.2006.05.022

Reddad, Z., Gerente, C., Andres, Y., and Le Cloirec, P. (2002). "Adsorption of several metal ions onto a low-cost biosorbent: Kinetic and equilibrium studies," *Environ. Sci. Technol.* 36(9), 2067-2073. DOI: 10.1021/es0102989

Santana, G. M., Trugilho, P. F., Borges, W. M. S., Bianchi, M. L., Paes, J. B., Nobre, J. R. C., and Morais, R. M. (2019). "Activated carbon from bamboo (*Bambusa vulgaris*) waste using CO_2 as activating agent for adsorption of methylene blue and phenol," *Ciênc. Florest.* 29(2), 769-778. DOI: 10.5902/1980509828648

Sarmah, S., Gogoi, S. B., Xianfeng, F., and Baruah, A. A. (2020). "Characterization and identification of the most appropriate nonionic surfactant for enhanced oil recovery," *J. Pet. Explor. Prod. Technol.* 10, 115-123. DOI: 10.1007/s13202-019-0682-1

Schukin, L. I., Kornnievin, M. V., Vartapetjan, R. S., and Beznisko, S. I. (2002). "Low temperature plasma oxidation of activated carbons," *Carbon* 40, 2021-2040.

Shan, D., Deng, S., Zhao, T., Wang, B., Wang, Y., Huang, J., Yu, G., Winglee, J., and Wiesner, M. R. (2016). "Preparation of ultrafine magnetic biochar and activated carbon for pharmaceutical adsorption and subsequent degradation by ball milling," *J. Hazard. Mater.* 305(2016), 156-163. DOI: 10.1016/j.jhazmat.2015.11.047

Sivakumar, V., Asaithambi, M., and Sivakumar P. (2012). "Physico-chemical and adsorption studies of activated carbon from agricultural wastes," *Adv. Appl. Sci. Res.* 3(1), 219-226.

Song, M., Jin, B. S., Xiao, R., Yang, L., Wu, Y. M., Zhong, Z. P., and Huang, Y. J. (2013). "The comparison of two activation techniques to prepare activated carbon from corn cob," *Biomass. Bioenerg.* 48(2013), 250-256. DOI: 10.1016/j.biombioe.2012.11.007

Strom, C. (2020). "Difference between charcoal and activated charcoal," (http://www.differencebetween.net/science/difference-between-charcoal-andactivated-charcoal/#ixzz6L49NFKRB).

Sumtong, P., Chollacoop, N., and Eiad-ua, A. (2017). "Effect of temperature and times by hydrothermal carbonization process from sawdust and bagasse for carbon material supporter," *J. Appl. Sci.* 16, 93-97. DOI: 10.14416/j.appsci. 2017.10.S14

Sun, Y., Paul, A., and Webley. (2008). "Preparation of activated carbons from corncob with large specific surface area by a variety of chemical activators and their application in gas storage," *Chem. Eng. J*. 162(3), 883-892. DOI: 10.1016/j.cej.2010.06.031

Sun, Y., Li, H., Li, G., Gao, B., Yue, Q., and Li, X. (2016). "Characterization and ciprofloxacin adsorption properties of activated carbons prepared from biomass wastes by H_3PO_4 activation," *Bioresource Technol.* 217, 239-244. DOI: 10.1016/j.biortech.2016.03.047

Thuan, T., Thinh, V., Quynh, P. V., Cong, H. T., Tam, D. T., and Bach, L.G. (2016). "Production of activated carbon from sugarcane bagasse by chemical activation with $ZnCl_2$: Preparation and characterization study," *Res. J. Chem. Sci.* 6(5), 42-47.

Wang, J., and Kaskel, S. (2012). "KOH activation of carbon-based materials for energy storage," *J. Mater. Chem.* 22, 23710-23725.

Wang, J., Nie, P., Ding, B., Dong, S. Y., Hao, X. D, Dou, H., and Zhang, X. G. (2017). "Biomass derived carbon for energy storage devices," *J. Mater. Chem.* A. 5(6), 24112428. DOI: 10.1039/C6TA08742F

Wang, B., Gao, B., and Wan, Y. (2018). "Comparative study of calcium alginate, ballmilled biochar, and their composites on aqueous methylene blue adsorption," *Environ. Sci. Pollut. Res.* 26, 11535-11541. DOI: 10.1007/s11356-018-1497-1

Welham, N, J., and Williams, J. S. (1998). "Extended milling of graphite and activated carbon," *Carbon* 36(9), 1309-1315. DOI: 10.1016/S0008-6223(98)00111-0

Welham, N. J., Berbenni, V., and Chapman, P. G. (2002). "Increased chemisorption onto activated carbon after ball-milling," *Carbon* 40(13), 2307-2315. DOI: 10.1016/S0008-6223(02)00123-9

Wu, Z., Qing, P., Guo, G., Shi, B., Hu, Q. 2019. "Effect of potassium-permanganate modification on the microstructure and adsorption property of activated carbon". *Mtaec* 9, 53(6), 853.

Yang, H., Yan, R., Chen, H., Lee, D. H., and Zheng, C. (2007). "Characteristics of hemicellulose, cellulose and lignin pyrolysis," *Fuel* 86(12-13), 1781-1788. DOI: 10.1016/j.fuel. 2006.12.013

Yang, J. B., Ling, L. C., Liu, L., Kang, F. Y., Huang, Z. H., and Wu, H. (2002). "Preparation and properties of phenolic resin based activated carbon spheres with controlled pore size distribution," *Carbon* 40(6), 911-916. DOI: 10.1016/S0008-6223(01)00222-6

Zhang, G., Sun, Y., Zhao, P., Xu, Y., Su, A. T., and Qu, J. (2017). "Characteristics of activated carbon modified with alkaline $KMnO_4$ and its performance in catalytic reforming of greenhouse gases CO_2/CH_4," *Journal of CO_2 Utilization* 20, 129-140. DOI: 10.1016/j.jcou.2017.05.013

Zhang, Q., Zeng, Y., Xiao, X., Deng, P., He, Q., and Zhang, T. (2019). "Investigation on the preparation and adsorption performance of bamboo fiber based activated carbon," *Fiber. Polym*. 20(2), 293-301. DOI 10.1007/s12221-019-8336-y

Article submitted: May 20, 2020; Peer review completed: July 12, 2020; Revised version received and accepted: September 10, 2020; Published: September 16, 2020.
DOI: 10.15376/biores.15.4.8303-8322